



ELSEVIER

Contents lists available at ScienceDirect

Cancer Letters

journal homepage: www.elsevier.com/locate/canlet

Original Articles

Downregulation of the circadian rhythm regulator HLF promotes multiple-organ distant metastases in non-small cell lung cancer through PPAR/NF- κ B signaling

Jiarong Chen^{a,b,1}, Aibin Liu^{c,d,1}, Zhichao Lin^{e,1}, Bin Wang^{a,f,g}, Xingxing Chai^{f,h}, Shasha Chen^{a,f,g}, Wenjie Lu^a, Mingzhu Zheng^a, Ting Cao^a, Meigong Zhongⁱ, Ronggang Li^j, Minyan Wu^k, Zhuming Lu^e, Wenguang Pang^e, Wenhai Huang^e, Lin Xiao^l, Daren Lin^b, Zhihui Wang^b, Fangyong Lei^b, Xiangmeng Chen^m, Wansheng Long^m, Yan Zhengⁿ, Qiong Chen^{c,d}, Jincheng Zeng^{f,g}, Dong Ren^{a,f}, Jun Li^a, Xin Zhang^{a,f,g,*}, Yanming Huang^{a,**}

^a Clinical Experimental Center, Jiangmen Key Laboratory of Clinical Biobanks and Translational Research, Jiangmen Central Hospital, Affiliated Jiangmen Hospital of Sun Yat-sen University, Jiangmen, 529030, China

^b Department of Oncology, Jiangmen Central Hospital, Affiliated Jiangmen Hospital of Sun Yat-sen University, Jiangmen, 529030, China

^c Department of Geriatrics, Respiratory Medicine, Xiangya Hospital, Central South University, Changsha, 410008, China

^d National Clinical Research Center for Geriatric Disorders, Xiangya Hospital, Central South University, Changsha, 410008, China

^e Department of Thoracic Surgery, Jiangmen Central Hospital, Affiliated Jiangmen Hospital of Sun Yat-sen University, Jiangmen, 529030, China

^f Dongguan Key Laboratory of Medical Bioactive Molecular Developmental and Translational Research, Guangdong Provincial Key Laboratory of Medical Molecular Diagnostics, Guangdong Medical University, Dongguan, 523808, China

^g Collaborative Innovation Center for Antitumor Active Substance Research and Development, Guangdong Medical University, Zhanjiang, 524023, China

^h Laboratory Animal Center, Guangdong Medical University, Zhanjiang, 524023, China

ⁱ Department of Pharmacy, Jiangmen Maternity and Child Health Care Hospital, Jiangmen, 529030, China

^j Department of Pathology, Jiangmen Central Hospital, Affiliated Jiangmen Hospital of Sun Yat-sen University, Jiangmen, 529030, China

^k Department of Basic Medicine, Guangdong Jiangmen Chinese Medical College, Jiangmen, 529030, China

^l Department of Radiotherapy Center, Jiangmen Central Hospital, Affiliated Jiangmen Hospital of Sun Yat-sen University, Jiangmen, 529030, China

^m Department of Radiology, Jiangmen Central Hospital, Affiliated Jiangmen Hospital of Sun Yat-sen University, Jiangmen, 529030, China

ⁿ Department of Research and Development, Research and Development Center for Molecular Diagnosis Engineering Technology of Human Papillomavirus (HPV) Related Diseases of Guangdong Province, Hybrbio Limited, Changzhou, 521021, China

ARTICLE INFO

Keywords:

NSCLC
Distant metastasis
Circadian rhythms regulator
Hepatic leukemia factor (HLF)
PPAR α
PPAR γ
NF- κ B pathway

ABSTRACT

Non-small cell lung cancer (NSCLC) is the leading cause of cancer-related death due to its early recurrence and widespread metastatic potential. Accumulating studies have reported that dysregulation of circadian rhythms-associated regulators is implicated in the recurrence and metastasis of NSCLC. Therefore, identification of metastasis-associated circadian rhythm genes is clinically necessary. Here we report that the circadian gene hepatic leukemia factor (HLF), which was dramatically reduced in early-relapsed NSCLC tissues, was significantly correlated with early progression and distant metastasis in NSCLC patients. Upregulating HLF inhibited, while silencing HLF promoted lung colonization, as well as metastasis of NSCLC cells to bone, liver and brain *in vivo*. Importantly, downexpression of HLF promoted anaerobic metabolism to support anchorage-independent growth of NSCLC cells under low nutritional condition by activating NF- κ B/p65 signaling through disrupting translocation of PPAR α and PPAR γ . Further investigations revealed that both genetic deletion and methylation con-

Abbreviations: ADC, lung adenocarcinoma; ANT, adjacent normal tissue; cDNA, complementary DNA; CNV, copy number variation; CNV&Methy Score, CNV and methylation score; ER, estrogen receptor; GAPDH, glyceraldehyde-3-phosphate dehydrogenase; H&E, hematoxylin and eosin stain; HLF, hepatic leukemia factor; IHC, immunohistochemistry; mRNA, messenger RNA; MSP, methylation-specific PCR; NSCLC, non-small cell lung cancer; PAR bZIP, proline and acid rich bZIP transcription factor family; PER, Period; Pol II, polymerase II; SD, standard deviation; SI, staining index; SQC, lung squamous cell carcinoma; STR, short tandem repeat; TCGA, The Cancer Genome Atlas

* Corresponding author. Jiangmen Central Hospital, Affiliated Jiangmen Hospital of Sun Yat-sen University, 23#, Haibang Street, Jiangmen, 529030, China.

** Corresponding author. Jiangmen Central Hospital, Affiliated Jiangmen Hospital of Sun Yat-sen University, 23#, Haibang Street, Jiangmen, 529030, China.

E-mail addresses: zhangx45@mail3.sysu.edu.cn (X. Zhang), huangyanming_jxy@163.com (Y. Huang).

¹ Author contributions: Jiarong Chen, Aibin Liu and Zhichao Lin contributed equally to this work.

<https://doi.org/10.1016/j.canlet.2020.04.007>

Received 21 December 2019; Received in revised form 1 April 2020; Accepted 7 April 2020

0304-3835/ © 2020 Elsevier B.V. All rights reserved.

tribute to downexpression of HLF in NSCLC tissues. In conclusion, our results shed light on a plausible mechanism by which HLF inhibits distant metastasis in NSCLC, suggesting that HLF may serve as a novel target for clinical intervention in NSCLC.

1. Introduction

Although multiple therapeutic strategies present favorable prospects for the treatment of primary NSCLC, NSCLC remains the leading cause of cancer-related death due to its early recurrence and widespread metastatic potential [1–3]. The most frequently seen metastatic sites of NSCLC include bone, brain and liver [2,3], which are found in as many as 56% of NSCLC patients at the time of initial diagnosis, subsequent follow-up and eventual autopsy [2]. When metastasized, formation of metastatic tumors produces metastasis-associated complications, including intractable pain, nerve compression syndrome, and even organ dysfunctions, causing significant morbidity and shorter survival. Therefore, further investigation of the metastatic-associated mechanisms is significantly crucial for the development of novel anti-metastatic therapeutic avenues for NSCLC.

As indicated by virtue of its nomenclature, circadian rhythm-associated molecules comprise a series of clock genes and proteins that play an important role in the regulation of sleep cycles [4]. Accumulating studies have reported that dysregulation of circadian rhythms-associated regulators is implicated in the tumorigenesis and metastasis of cancers through varying mechanisms [5–7]. Recently, considerable attention has been made on the roles of circadian clock genes in NSCLC. For example, overexpression of *CRY2*, *BMAL1*, and *RORA* in combination with downexpression of *TIMELESS* and *NPAS2* was associated with a favorable prognosis in lung adenocarcinoma, whereas high expression of *DEC1* and *TIMELESS* predicted poor overall survival in squamous cell NSCLC [8]. Furthermore, several members of Period (PER) protein family, including *PER1-3*, were found to be down-regulated in NSCLC, which significantly correlated with poor clinicopathological features, and predicted a shorter survival in NSCLC patients [9]. This negative effect of *PER2* on NSCLC was mediated by increased expression of the tumor suppressor genes, *BAX*, *TP53* and *TP21* by repressing *PI3K/AKT/mTOR* signaling pathway [10,11]. However, the clinical significance and role of deregulation of circadian genes in early relapse and distant metastasis of NSCLC remains largely unknown.

By analyzing multiple circadian-associated regulators in the NSCLC datasets from The Cancer Genome Atlas (TCGA) and our previous integrative RNA expression profiles from the ArrayExpress (AE-meta) [12], in the current study, we identified a circadian gene-hepatic leukemia factor (HLF), a member of the proline and acidic amino acid-rich basic leucine zipper transcription factor family (PAR bZIP) [13,14], was dramatically reduced in early-relapsed NSCLC tissues, which was significantly correlated with early progression and distant metastasis in NSCLC patients. Gain and loss of function experiments showed that upregulating HLF inhibited, while silencing HLF promoted lung colonization, as well as metastasis of NSCLC cells to bone, liver and brain *in vivo*. Our results further revealed that downexpression of HLF promoted anaerobic metabolism to support anchorage-independent growth of NSCLC cells under low nutritional condition by activating *NF-κB/p65* signaling via disrupting translocation of *PPARα* and *PPARγ*. Further investigation implied that both genetic deletion and methylation contribute to downexpression of HLF in NSCLC tissues. Collectively, our results explore a plausible mechanism by which HLF inhibits relapse and metastasis in NSCLC, suggesting that HLF may serve as a novel target for clinical intervention against NSCLC.

2. Materials and methods

2.1. Cells and cell culture

Human lung adenocarcinoma cell lines Calu-3, NCI-H1975, NCI-H1395, lung squamous carcinoma cell lines NCI-H520, NCI-H226, SK-MES-1, NSCLC cell lines A549, NCI-H460, NCI-H1299, NCI-H292 and non-cancerous immortalized lung bronchial epithelial cells BEAS-2B, normal lung fibroblast cells WI-38 were obtained from Shanghai Chinese Academy of Sciences cell bank (Shanghai, China) and Procell (Wuhan, China). BEAS-2B was grown in Bronchial Epithelial Cell Growth Medium BulletKit (BEGM, Lonza, Switzerland), WI-38, Calu-3 and SK-MES-1 were cultured in Eagle's Minimum Essential Medium (MEM, Gibco, USA), NCI-H1975, NCI-H1395, NCI-H460, NCI-H1299, NCI-H292, NCI-H520 and NCI-H226 were maintained in RPMI-1640 (Gibco, USA), and A549 was grown in F12K Medium (Gibco, USA). All cell lines, except for BEAS-2B, were supplemented with 10% fetal bovine serum (Gibco, USA). All cell lines were authenticated using short tandem repeat (STR) profiling by HybriBio Limited (China). Cells were incubated at 37 °C in a humidified atmosphere with 5% CO₂. A low nutritional condition was induced by culturing cells under low-serum (1%) and low-glucose (1 g/L) conditions [15]. Anoikis induction assay Cells were kept in suspension by using poly-HEMA (Sigma-Aldrich, USA) coated plates to prevent adhesion, in anoikis induction assay [16]. After 48 h of suspension, cells were harvested for apoptosis analysis by flow cytometry.

2.2. Patients and tumor tissues

The 11 paired lung adenocarcinoma (ADC) tissues, 8 paired lung squamous cell carcinoma (SQC) tissues and 1 lung adenosquamous carcinoma tissues and the 20 corresponding matched adjacent tumor normal tissues were obtained during surgery and the clinicopathological features of the patients are summarized in Supplemental Table 1. A total of 406 HLF immunohistochemistry detected, archived lung samples, including 64 benign lung disease lesions, 204 ADC tissues, 112 SQC tissues and 26 other subtypes of NSCLC, were obtained during surgery or needle biopsy. The clinicopathological features of the 64 patients with benign lung disease are summarized in Supplemental Table 2 and the 342 patients with NSCLC are summarized in Supplemental Table 3. All tissues were collected from the Affiliated Jiangmen Hospital of Sun Yat-sen University (Guangdong, China) between January 2008 and December 2018. Patients were diagnosed based on clinical and pathological evidence, and the specimens were immediately snap-frozen, liquid nitrogen tanks stored, or 0.6 μm frozen section, –86 °C refrigerator stored. For the use of these clinical materials for research purposes, prior patients' consents and approval from the Institutional Research Ethics Committee of the Affiliated Jiangmen Hospital of Sun Yat-sen University were obtained (Approval number: 2019–002). The proportions of tumor vs. non-tumor in hematoxylin and eosin (H&E) staining tissue samples were evaluated by the two independent professional pathologists. The tumor proportions in all clinical NSCLC tissue samples analyzed in this study exceeded 75% in real-time PCR analysis and western blotting.

2.3. Immunohistochemistry

The immunohistochemistry procedure and scoring of HLF expression were performed as previously described [12]. Briefly, the slides of frozen section were 4% formalin-fixed 10 min, antigen-retrieved in

TE (pH 9.0) buffer 10 min by microwave heating, blocked by hydrogen peroxide and goat serum respectively, and incubated overnight at 4 °C in a humidified chamber with the antibodies diluted 1:100 in Antibody Diluent (Abcam, USA). After incubation, slides were washed in TBS/0.05% Tween 20, incubated with biotin-conjugated secondary antibody (Proteintech, China) and peroxidase-conjugated streptavidin (Proteintech, China) 30 min at 37 °C respectively, stained by 3,3'-Diaminobenzidine (DAB) Enhanced Liquid Substrate System (Sigma-Aldrich, USA). Staining index (SI) given by the two independent investigators were averaged for further comparative evaluation of HLF expression. Tumor cell proportion was scored as follows: 0 (no positive tumor cells); 1 (< 10% positive tumor cells); 2 (10–35% positive tumor cells); 3 (35–70% positive tumor cells) and 4 (> 70% positive tumor cells). Staining intensity was graded according to the following criteria: 0 (no staining); 1 (weak staining, light yellow); 2 (moderate staining, yellow brown) and 3 (strong staining, brown). SI was calculated as the product of staining intensity score and the proportion of positive tumor cells. Based on this method of assessment, HLF expression in lung tumor samples was evaluated by the SI, with scores of 0, 1, 2, 3, 4, 6, 8, 9 or 12. SI score 4 was the median of all sample tissues SI. High and low expression of HLF were stratified by the follow criteria: The $SI \leq 4$ was used to define tumors with low expression of HLF, and SI score of > 4 as tumors with high expression of HLF.

2.4. RNA extraction, reverse transcription, and real-time PCR

Total RNA from tissues or cells was extracted using RNA Isolater (Vazyme, China) according to the manufacturer's instructions. Messenger RNA (mRNA) was reverse transcribed of total mRNA using the HiScript III 1st Strand cDNA Synthesis Kit (Vazyme, China) according to the manufacturer's protocol. Complementary DNA (cDNA) was amplified and quantified on ABI 7500 Fast system (Thermo-Fisher, USA) using ChamQ Universal SYBR qPCR Master Mix (Vazyme, China). The primers were provided in Supplemental Table 4, and were synthesized and purified by Biosune Biotechnology Co., Ltd (China). Real-time PCR was performed according to the manufacturer's protocol, and glyceraldehyde-3-phosphate dehydrogenase (GAPDH) was used as endogenous controls for mRNA. Relative fold expressions were calculated with the comparative threshold cycle ($2^{-\Delta\Delta Ct}$) method, as described previously [12]. The copy number variation (CNV) of each sample of NSCLC was examined using real time PCR primer Hs01509093_cn through TaqMan copy number assay. TaqMan Copy Number Reference Assay RNase P (Thermo-Fisher, USA) and TaqMan Fast Advanced Master Mix (Thermo-Fisher, USA) were used as the loading control and amplification kit. Copy number were calculated with the comparative threshold cycle ($2^{-\Delta\Delta Ct}$) method, as described previously [17], and the monocytes in the blood from healthy donor was used as reference.

2.5. Quantitative methylation-specific PCR (MSP) assay

DNA from NSCLC samples and cells was extracted using the FastPure Cell/Tissue DNA Isolation Mini Kit (Vazyme, China) according to the manufacturer's instructions; then, DNA was subjected to bisulphite conversion with the EpiArt DNA Methylation Bisulfite Kit (Vazyme, China). Methylation specific high resolution melting curve analysis was further performed using the EvaGreen High Resolution Melting (HRM) Assay Kit (Tiangen, China). The primers used to detect methylation levels were provided in Supplemental Table 5. Positive control of cg01392772(C), cg05452524(C), cg02383154(C), cg01185682(C) and cg01451391(C), and negative control of those sites with (T) were constructed into pMD20-T vector plasmid using Mighty TA-cloning Kit (TaKaRa, China), and standard samples was prepared according to 1:0, 3:1, 1:1, 1:3, and 0:1 with positive and negative control vector plasmid. Methylation level was compared with standard samples by HRM curve, as described previously [18], and defined the methylation level equal to or greater than 75% as “fully methylated”,

equal to or less than 25% as “fully unmethylated”, and between 25% and 75% as “partially methylated”.

2.6. Plasmid, small interfering RNA and transfection

The human HLF gene was PCR-amplified from genomic DNA and cloned into the Ubi-MCS-3FLAG-SV40-puromycin lentiviral vector (CV064, Genechem, China). The short hairpin (shRNA) RNA for human HLF was cloned into a hU6-MCS-CBh-gcGFP-IRES-puromycin lentiviral vector (GV493, Genechem, China), and the list of primers used in clone reactions was presented in Supplemental Table 6. Transfection of plasmids was performed using Lipofectamine 3000 reagent (Invitrogen, USA) according to the manufacturer's instructions. Stable cell lines expressing HLF, shHLF#1 or shHLF#2 were generated by filtered-lentivirus infection using HEK293T cells (Guangzhou Jet Bio-Filtration Co., Ltd.), and selected with 0.5 mg/L puromycin (Sigma-Aldrich, USA) for 10 days, as described previously [12]. The luciferase reporter plasmids of multiple signaling pathways used in our previous study were used to examine the effect of HLF on activity of these signaling [19]; pGL6-luc (Beyotime, China) and pGL6-TA-luc (Beyotime, China) were using as control vector, and pRL-SV40-N (Beyotime, China) was using as external reference.

2.7. Western blotting analysis

Nuclear/cytoplasmic fractionation was separated by using Cell Fractionation Kit (Cell Signaling Technology, USA) according to the manufacturer's instructions, and the whole cell lysates were extracted using RIPA Buffer (Beyotime, China). Western blot was performed according to a standard method, as previously described [12]. Briefly, the cell lysates were loaded with 10% Loading Buffer (Beyotime, China) and heated for 5 min at 100 °C. Equal quantities of denatured protein samples were resolved on 8–16% SDS-polyacrylamide gels, and then transferred onto Immobilon-PSQ PVDF membranes (Millipore, USA). After blocking with 5% non-fat dry milk in TBS/0.05% Tween 20, membranes were incubated with a specific primary antibody, followed by a horseradish peroxidase-conjugated secondary antibody (Thermo-Fisher, USA). Proteins were visualised using BeyoECL Plus reagents (Beyotime, China). Antibodies against HLF (Invitrogen, USA), PPAR α (Invitrogen, USA), PPAR β/δ (Abcam, USA) PPAR γ (Invitrogen, USA), NF- κ B p65 (Cell Signaling Technology, USA), p-NF- κ B p65 (Ser536, Cell Signaling Technology, USA), I κ B α (Cell Signaling Technology, USA), p-I κ B α (Ser32/36, Cell Signaling Technology, USA) were using specific primary antibody, and α -tubulin and p84 which detected by anti- α -tubulin (Proteintech, China) or anti-p84 antibody (Invitrogen, USA) as the loading control.

2.8. Cell Counting Kit-8 analysis and colony formation assay

For Cell Counting Kit-8 analysis, cells (0.5×10^3) were seeded into 96 well plates and stained at the indicated time point with 100 μ l Cell Counting Kit-8 (CCK-8; Dojindo, Japan) dye for 1 h at 37 °C, followed by the absorbance was measured at 450 nm, with 650 nm used as the reference wavelength. For colony formation assay, cells (0.5 – 1.0×10^3) were plated into six well plates and cultured for 7–10 days. Colonies were fixed for 15 min with 10% formaldehyde, stained with 1.0% crystal violet for 30s, and washed by water.

2.9. Anchorage-independent growth assay

Cells (3×10^3) were plated in 6 well plates in 2 ml complete medium containing 0.32% agar (Sigma-Aldrich, USA). The agar-cell mixture was plated as a top layer onto a bottom layer comprising 0.66% complete medium agar mixture. Additional media was added to the cultures once per week, and after two weeks culture, colony size was measured using an ocular micrometer and colonies > 0.1 mm (or > 50 cells) in diameter were counted.

2.10. Flow cytometric analysis

Flow cytometric analyzed of apoptosis were used the Annexin V-FITC/PI Apoptosis Detection Kit (KeyGEN, China), and was presented as protocol described [18]. Briefly, cells were dissociated with trypsin and resuspended at 1×10^7 cells/ml in binding buffer with 500 μ l/ml Annexin V-FITC and 500 μ l/ml PI. The cells were subsequently incubated for 15 min at room temperature, and then were analyzed by Gallios flow cytometer (Beckman Coulter, USA). The cell's inner mitochondrial membrane potential ($\Delta\psi$ M) was detected by flow cytometric using JC-1 Staining Kit (KeyGEN, China), and was presented as protocol described [18]. Briefly, cells were dissociated with trypsin and resuspended at 1×10^7 cells/ml in Assay Buffer, and then incubated at 37 °C for 15 min with 100 μ l/ml JC-1. Before analyzed by flow cytometer, cells were washed twice by Assay Buffer, and filtered by cell mesh. Flow cytometry data were analyzed using FlowJo VX software (TreeStar Inc., USA).

2.11. Dual luciferase report experiments

Cells (5×10^5) were plated in 60-mm cell culture dishes, proliferating to 60–80% confluence after 24 h of culture, and the reporter constructs were transfected into cells using Lipofectamine 3000. After 12h incubation, the transfection medium was replaced; cells were harvested and washed with PBS, and lysed with lysis buffer. The cell lysates were analyzed immediately using Synergy 2 microplate system (BioTek, USA). Luciferase and Renilla luciferase were measured using a Renilla-Lumi Luciferase Reporter Gene Assay Kit (Beyotime, China) according to the manufacturer's instructions. The luciferase activity of each lysate was normalized to Renilla luciferase activity. The relative transcriptional activity was converted into fold induction above the control group value.

2.12. Metabolic assays

Cellular glucose up-taking, lactate excretion, LDH activity, ATP contents, triglycerides contents, free fatty acids contents and total protein contents were measured using the Glucose Uptake Colorimetric Assay Kit (Abcam, USA), the Lactate Colorimetric Assay Kit (Abcam, USA), the Lactate Dehydrogenase Assay Kit (Abcam, USA), the ATP Detection Assay Kit (Abcam, USA), the triglyceride Assay Kit (Abcam, USA), BCA Total Protein Assay Kit (Jiancheng Bioengineering Institute, China) and Free Fatty Acid Quantification Assay Kit (Abcam, USA), according to the manufacturer's instructions, respectively. Briefly, to measure cellular uptake of glucose, indicated cells were cultured in low nutrition conditions for 72 h and then starved in KRPH/2% BSA for 40 min and treated with 2-DG for 20 min, followed by cell lysate preparation with extraction buffer and freezing at -86 °C. The frozen samples were thawed to degrade endogenous NAD(P) and processed for measurement of 2-DG6P at OD 412 nm in a microplate reader. To measure lactate production, indicated cells were cultured in low nutrition conditions for 72 h, culture medium was collected and mixed with Lactate Assay Buffer (50 μ l/well) in a 96-well plate. Then, 50 μ l of Reaction Buffer was added to each well for 30 min at room temperature. Absorbance was measured at OD 450 nm in a microplate reader. Lactate concentrations were determined on basis of the lactate standards and normalized to cells number (1×10^6) of each sample. To measure LDH activity, indicated cells were cultured in low nutrition conditions for 72 h, a total of 1×10^6 cells were harvested by centrifugation at $13,000 \times g$ and 4 °C for 10 min, and then homogenized with three volumes of cold assay buffer and centrifuged at 4 °C at $10,000 \times g$ for 15 min to eliminate insoluble material. Absorbance was measured at OD 450 nm in a microplate reader. LDH activity was estimated using a standard curve with NADH as a reference. To measure ATP contents, indicated cells were cultured in low nutrition conditions for 72 h, 100 μ l of the cell lysate was mixed with 100 μ l of ATP reaction

mix and incubated for 30 min. Absorbance was measured at OD 450 nm in a microplate reader. To measure cellular triglycerides, indicated cells were cultured in low nutrition conditions for 72 h, indicated cells were collected and lysed. A total of 50 μ l of gradient standard and 10 μ l of the sample measured at OD 570 nm in a microplate reader, and the absorbance of the sample was calculated according to the standard curve and normalized by the cells number (1×10^8) of each sample. To measure cellular free fatty acids, indicated cells were cultured in low nutrition conditions for 72 h, harvested and homogenized in 200 μ l chloroform/Triton X-100 by pipetting up and down, followed by incubate on ice for 10–30 min. Spin the extract at $13,000 \times g$ and 4 °C for 10 min, then collect organic phase (lower phase), air dry at 50 °C in a fume hood to remove chloroform. Dissolve the dried lipids in 200 μ l Fatty Acid Assay Buffer by vortexing extensively for 5 min. Add 2 μ l ACS reagent and incubate for 30 min at 37 °C. Next, 50 μ l of reaction mix was added and incubate at 37 °C for 30 min protected from light. The absorbance at 570 nm was measured immediately afterwards on a microplate reader.

2.13. Animal study

Xenograft tumor experiments were approved by the Institutional Animal Care and Use Committee of Guangdong Medical University (Approval number: GDY1902006). At least 6 or 8 nude mice per group were used to ensure the adequate power and each mouse with different weight was randomly allocated. For tail vein injection, $1-2 \times 10^6$ cells in 100 μ l PBS were injected into the lateral tail vein of BALB/c-nu mice (4–6 wk old; 18–20 g). The intracardiac model of metastasis was performed as previously described [20]. Briefly, $1-2 \times 10^5$ cells were resuspended in 100 μ l PBS and inoculated into the left cardiac ventricle of BALB/c-nu mice by a 28.5 G insulin syringe. Mice were monitored twice weekly and were sacrificed by cervical dislocation dependent on survival time. Lungs, brains, livers and limbs of each group of mice were dissected and fixed with 4% paraformaldehyde. Limbs were decalcified by gentle shaking in TE decalcifying solution (pH 7.4) for 4 wks. All the tissues were finally paraffin embedded and subjected to hematoxylin and eosin (H&E). For detection of HLF in mice lung of tail vein injection model, tissues were performed 0.6 μ m frozen section and follow the same protocol as clinical sample. The tumor cell number was evaluated in 9 random fields (mm^2) of the H&E tissues under 20X magnification using M8 Digital Microscopy (Precipoint, Germany). Then, the cell number in each field was added up to be used for analysis.

2.14. High throughput data processing and visualization

The clinical profile of NSCLC dataset, RNA sequencing profile, copy number variation profile and methylation array profile were downloaded from The Cancer Genome Atlas (TCGA; <https://tcga-data.nci.nih.gov/tcga/>) and the analysis for RNA sequencing profile was used Excel 2016 (Microsoft, USA) and GraphPad 5 (GraphPad Software Inc., USA) software. The 17 RNA sequencing profiles of non-small cell lung cancer based on Affymetrix U133 Plus2.0 microarray were downloaded from ArrayExpress (<http://www.ebi.ac.uk/arrayexpress/>). Integrated analysis of all data collected from ArrayExpress using YuGene program was described previously [12,21], including 340 normal lung tissues and 2032 NSCLC tissues, and the integrative expression profile of NSCLC was named for AE-meta dataset. The expression values were normalized by z-score, and performed on heat map by MeV4.9 software (<http://www.tm4.org/>). In TCGA, AE-meta and KM Plotter datasets, the median of HLF expression in all NSCLC tissues was used cutoff value to stratify high and low expression of HLF.

Copy number variation profile for TCGA of SNP6.0 microarray was analyzed the dataset by GISTIC2.0 software as described previously [18], and defined the CNV number 2 as “Diploid”, greater than 2 as “Gain” and less than 2 as “Deletion”. Methylation array profile for

TCGA of 450 K Methylation microarray was procure the β -value (representing methylation level) of the 16 HLF-related probe number, and calculate the differential β -value between the adjacent normal tissue (ANT) and NSCLC tissues. Defined the β -value equal to or greater than 0.6 as “fully methylated”, equal to or less than 0.2 as “fully

unmethylated”, and between 0.2 and 0.6 as “partially methylated”, according to the manufacturer's instructions by Illumina and UCSC Genome Browser (<http://genome.ucsc.edu/>).

Gene Set Enrichment Analysis (GSEA) was performed using GSEA 3.0 (<http://www.broadinstitute.org/gsea>) as previously described [17].

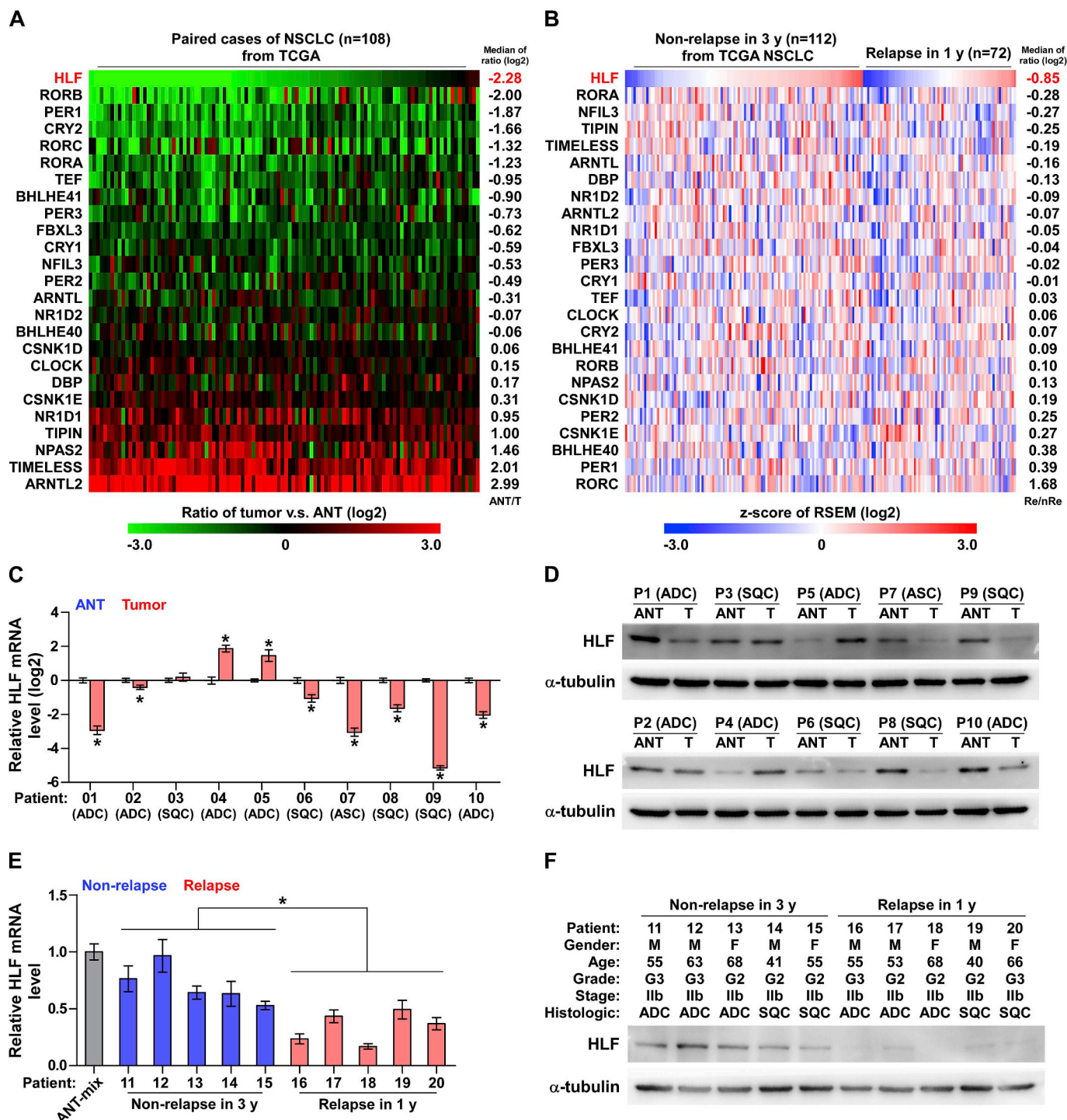
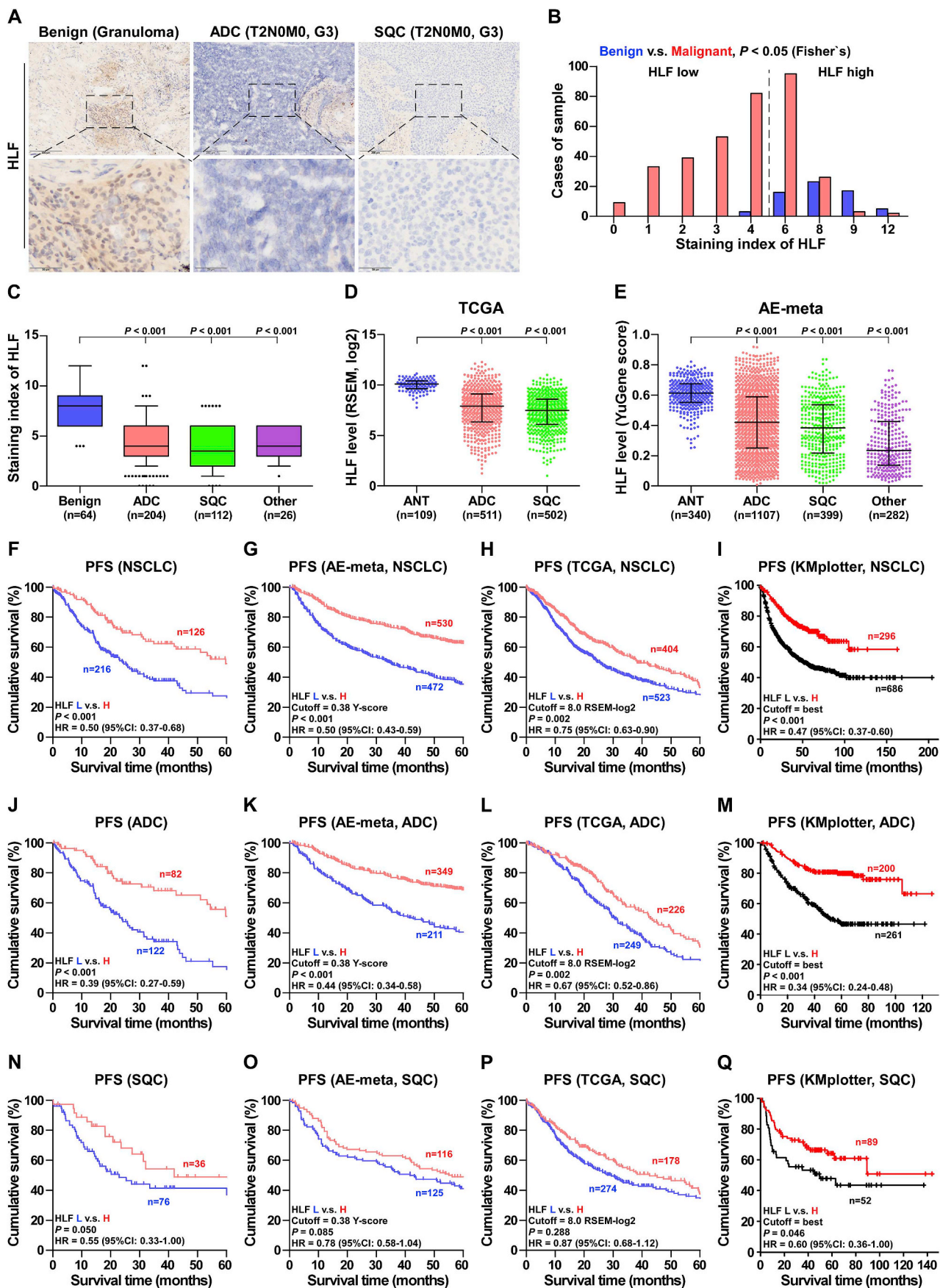


Fig. 1. HLF is downregulated in early relapsing NSCLC tissues. (A) Expression level of circadian genes in NSCLC (LC) tissues compared with those in the adjacent normal tissues (ANT) (n = 108) by analyzing the dataset of NSCLC from TCGA. (B) Expression level of circadian genes in early relapsing NSCLC tissues (relapse within 1 year, n = 72) compared with those in non-relapse NSCLC tissues (non-relapse within 3 year, n = 112) by analyzing the dataset of NSCLC from TCGA. (C) Real-time PCR of HLF mRNA levels in paired NSCLC tissues compared with matched ANT. Transcript levels were normalized to GAPDH expression. *P < 0.05. (D) Western blotting analysis of HLF protein levels in paired NSCLC tissues compared with matched ANT. α -Tubulin served as the loading control. (E and F) mRNA expression and protein levels of HLF in 1-year relapsing NSCLC tissues (n = 5) compared with 3-year non-relapsing NSCLC tissues (n = 5). Transcript levels were normalized to GAPDH expression. *P < 0.05. α -Tubulin served as the loading control.



(caption on next page)

Fig. 2. Downexpression of HLF correlates with advanced clinicopathological features and early progression in NSCLC. (A) Typical pictures of immunohistochemical staining of HLF in different subtypes of NSCLC and benign lung disease tissues. (B) The case number of different immunohistochemical staining index of HLF in malignant NSCLC tissues and benign lung disease tissues (benign lung disease tissues, $n = 64$; ADC, $n = 204$; SQC, $n = 112$; other subtypes of NSCLC, $n = 26$). (C) Immunohistochemical staining index of HLF in different subtypes of NSCLC compared with benign lung disease tissues. (D) HLF expression was downregulated in ADC and SQC compared with adjacent normal tissues (ANT) from TCGA (ANT, $n = 109$; ADC, $n = 511$; SQC, $n = 502$). (E) HLF expression was downregulated in different subtypes of NSCLC compared with adjacent normal tissues (ANT) from AE-meta (ANT, $n = 340$; ADC, $n = 1107$; SQC, $n = 399$; other NSCLC, $n = 282$). (F to I) Progression-free survivals of NSCLC patients with low HLF expression compared with those with high HLF expression in our samples, AE-meta, TCGA and Kaplan-Meier Plotter profiles. (J to M) Progression-free survivals of ADC patients with low HLF expression compared with those with high HLF expression in our samples, AE-meta, TCGA and Kaplan-Meier Plotter profiles. (N to Q) Progression-free survivals of SQC patients with low HLF expression compared with those with high HLF expression in our samples, AE-meta, TCGA and Kaplan-Meier Plotter profiles.

Briefly, we first downloaded the mRNA sequencing dataset of lung cancer from TCGA and procure the expression value of the corresponding genes from the Level 3 data of each sample (The unit was RNA-Seq by Expectation Maximization, RSEM); analyze the log₂ value of each sample using Excel 2016. GSEA was performed with RNA sequencing dataset of lung cancer from TCGA as Expression dataset. The high and low expression level of HLF was stratified by the medium expression level of HLF in all lung cancer tissues. Gene set was performed by Molecular Signatures Database v7.0 (<http://software.broadinstitute.org/gsea/msigdb>) (all processing parameters as the default).

2.15. Statistical analysis

All values are presented as means \pm standard deviation (SD). Significant differences were determined using GraphPad Prism 5 software. Student's t-test was used to determine statistical differences between two groups. One-way ANOVA was used to determine statistical differences between multiple testing, and post test using Tukey test to compare all pairs of groups. The chi-square test was used to analyze the relationship between HLF expression and clinicopathological characteristics. Survival curves were plotted using the Kaplan-Meier method and compared by log-rank test. $P < 0.05$ was considered significant. All the repetitive experiments were repeated three times.

3. Results

3.1. HLF is downregulated in early relapsing NSCLC tissues

Since disruption of the circadian rhythm has been extensively implicated in the relapse and metastasis in a variety of human cancers [14], including NSCLC [22], the clinical significance of circadian-associated molecules in NSCLC seized our great momentum. By analyzing the expression levels of multiple circadian-associated regulators in the RNA sequencing dataset of NSCLC from TCGA, we found that expression levels of HLF was dramatically reduced in NSCLC tissues compared with that in the adjacent normal tissues (ANT) (Fig. 1A). Importantly, HLF was also the most downregulated one of all circadian-associated regulators in early-relapsed NSCLC tissues compared with non-relapsed NSCLC tissues (Fig. 1B). Consistently, results from our previous integrative data profile of NSCLC based on Affymetrix U133 Plus2.0 microarray (AE-meta) combined with TCGA analysis further showed that HLF expression was significantly downregulated in NSCLC tissues (Supplemental Fig. 1A and B), and was further reduced in early-relapsed NSCLC tissues (Supplemental Fig. 1C and D). Real-time PCR and Western blotting analysis revealed that the mRNA and protein levels of HLF were reduced in 7/10 paired NSCLC tissues compared with those in their matched ANT (Fig. 1C and D). Furthermore, HLF expression was significantly downregulated in early-relapsed NSCLC tissues compared with non-relapsed NSCLC tissues (Fig. 1E and F). Taken together, our findings in combination with the results of several publicly available NSCLC datasets indicated that HLF is downregulated in NSCLC tissues, especially in those with early relapse.

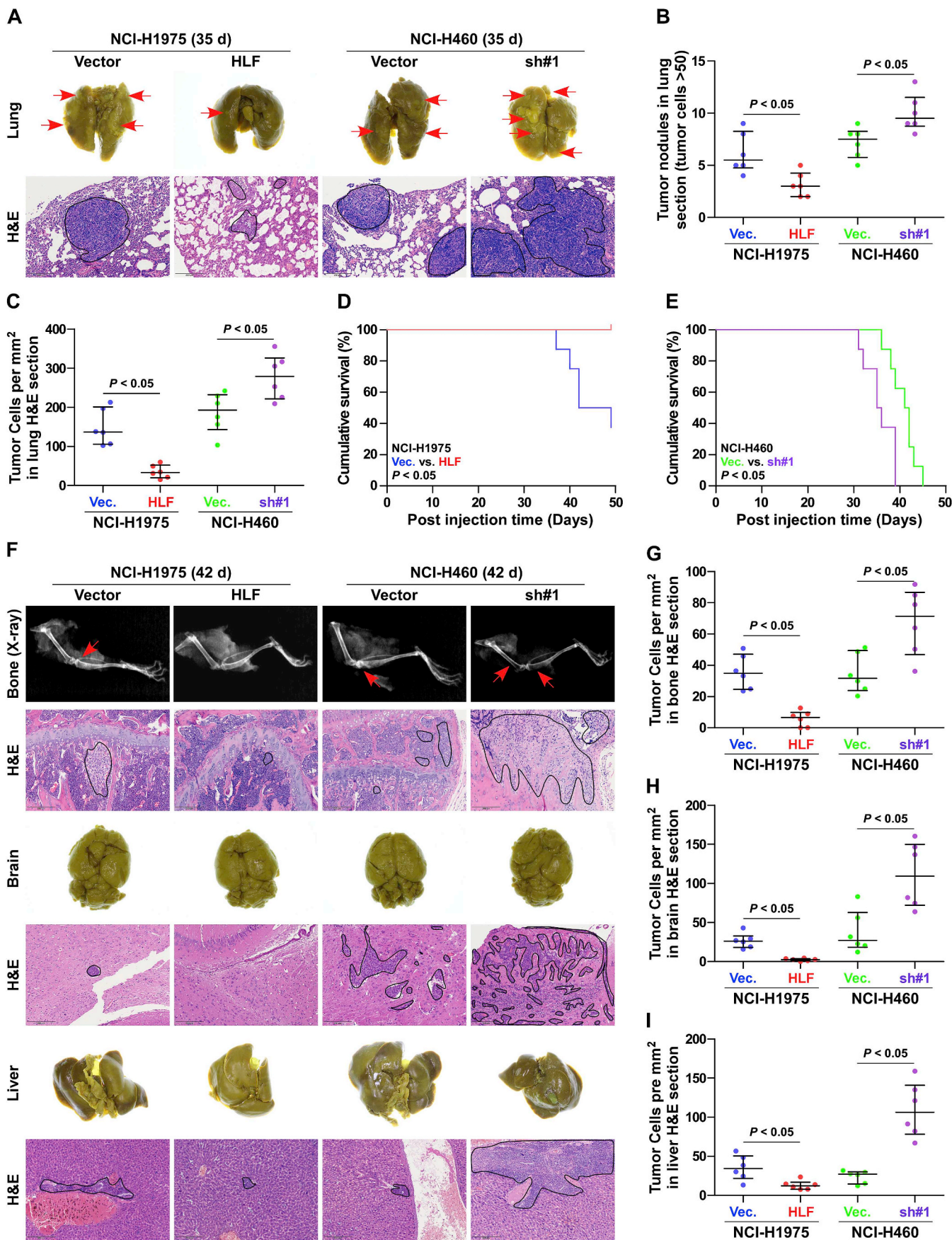
3.2. Downexpression of HLF correlates with advanced clinicopathological features and early progression in NSCLC

HLF expression was further examined in tissues from 64 benign lung disease tissues, 204 lung adenocarcinoma (ADC), 112 lung squamous carcinoma (SQC) and 26 other subtypes of NSCLC by immunohistochemical staining. Compared with expression of HLF in lung benign tumor tissues, it was differentially downregulated in ADC, SQC and other NSCLC tissues (Fig. 2A–C), which was further supported by the findings from the NSCLC datasets from TCGA and AE-meta (Fig. 2D and E). Kaplan-Meier survival analysis further revealed that NSCLC patients with low HLF expression predicted poorer progression-free survivals compared with those with high HLF expression (Fig. 2F), which was consistent with the findings from TCGA, AE-meta and Kaplan-Meier Plotter profiles (Fig. 2G–I). Likewise, shorter progression-free survivals were observed in ADC and SQC patients with low HLF expression (Fig. 2J–Q). Furthermore, expression levels of HLF decreased gradually with advanced clinical grade (Supplemental Fig. 1E and F; Supplemental Table 7) and stages (Supplemental Fig. 1G–I; Supplemental Table 7).

It is well known that advanced tumor grade and stage are significantly associated with expedited progression of NSCLC. Our results above showed that downexpression of HLF was correlated with advanced clinical grade and stage, as well as poorer progression-free survival. Therefore, to dissect the individual effect of advanced tumor grade and stage on poorer progression-free survival in NSCLC patients due to downexpression of HLF, NSCLC patients were first stratified into different subgroups of grade I to III and stage I to IV respectively. As shown in Supplemental Fig. 2A–F, NSCLC patients with low expression of HLF exhibited shorter progression-free survival in the same pathological grade compared with those with high expression of HLF. Consistently, similar findings were also identified in the setting of NSCLC patients with the same clinical stage according to multiple independent datasets, including our sample (Supplemental Fig. 2G and H), TCGA (Supplemental Fig. 2I and J), AE-meta (Supplemental Fig. 2K and L) and Kaplan-Meier Plotter (Supplemental Fig. 2M – O). Collectively, our findings demonstrated that downexpression of HLF significantly and positively correlates with early progression and advanced clinicopathological features in NSCLC patients.

3.3. Downexpression of HLF promotes early local relapse and multiple organs distant metastasis in NSCLC

Further investigation revealed that downexpression of HLF was positively associated with shorter local relapse-free survival and distant metastasis-free survival in NSCLC patients (Supplemental Fig. 3A–D). Similarly, poorer local relapse-free survival and distant metastasis-free survival were found in ADC patients with downexpression of HLF (Supplemental Fig. 3E–H) as well as in SQC patients (Supplemental Fig. 3I–L). To further determine the role of HLF in local lung colonization and distant metastasis of NSCLC cells, HLF expression was first examined in multiple different subtypes of NSCLC cell lines. As shown in Supplemental Fig. 4A and B, mRNA and protein levels of HLF were differentially downregulated in NSCLC cells compared with those in non-cancerous immortalized lung bronchial epithelial cells BEAS-2B



(caption on next page)

Fig. 3. Silencing HLF expression enhanced formation of local and distant metastatic tumors. (A) Lung metastases in mice were confirmed by H&E staining. Arrows indicate the metastatic colonization of tumor cells. (B) The numbers of lung tumor nodules with tumor cells > 50 in lung section of each group was counted and presented as the median values \pm quartile values. * $P < 0.05$. (C) The numbers of lung tumor cells per mm^2 in lung H&E sections in each group were counted and presented as the median values \pm quartile values. * $P < 0.05$. (D and E) Kaplan-Meier survival curves for mice after tail veins injection of the indicated NSCLC cells. * $P < 0.05$. (F to I) Metastatic tumors and H&E staining in distant organs of bone, brain and liver. Arrows indicate the metastatic colonization of tumor cells in distant organs (F). The numbers of tumor cells per mm^2 in H&E sections in each group were counted and presented as the median values \pm quartile values (G to I). * $P < 0.05$.

and normal lung fibroblast cells WI-38. We further constructed HLF-stably overexpressing NCI-H1975 (H1975) and NCI-H520 (H520) lung carcinoma cells that expressed the lowest endogenous levels of HLF among all the NSCLC cell lines, and endogenously knocked down HLF expression in NCI-H460 (H460) and NCI-H1299 (H1299) cells, both of which expressed the highest endogenous levels of HLF (Supplemental Fig. 4C and D).

The lung colonization and outgrowth ability of NSCLC cells were investigated in a mouse model of tail veins. As shown in Fig. 3A–D and Supplemental Fig. 4E, upregulating HLF significantly repressed the tumorigenesis of H1975 cells in the lungs, as indicated by the decreased formation of lung nodule, reduced number of cancer cells per mm^2 and the extended cumulative survival. Conversely, silencing HLF had the opposite effect in H460 cells (Fig. 3A–C, E and Supplemental Fig. 4E). It was noteworthy that altered expression of HLF not only had an influence on the formation of large lung nodule (defined as > 50 tumor cells in the analyzed tumor section) (Fig. 3B), but also affected on the formation of small lung nodule (defined as 5–50 tumor cells in the analyzed tumor section) (Supplemental Fig. 4E), supporting the notion that HLF plays an important role in both early colonization of tumor cells and subsequent outgrowth in the lungs. Finally, the corresponding high and low HLF expression level was further confirmed in the tumor tissues from the mice injected with HLF-stably overexpressing H1975 cells and downexpressing H460 cells compared with those in the vector at the end of the experiments (Supplemental Fig. 4F).

Then, a mouse model of left cardiac ventricle inoculation *in vivo* was used to examine the effect of HLF on the distant metastasis ability in NSCLC, where vector/NCI-H1975, HLF overexpressing NCI-H1975, vector/NCI-H460 and HLF sh#1/NCI-H460 cells were inoculated into the left cardiac ventricle of the mice. After 6 weeks of cells inoculation, the tibiae, brain and liver tissues were collected from the mice and processed using H&E staining. As shown in Fig. 3F–I and Supplemental Fig. 4G, we detected fewer and smaller metastatic tumors in distant organs, including bone, brain and liver, as well as the prolonged cumulative survival in the HLF-overexpressing mice group than the vector group. By contrast, silencing HLF significantly enhanced formation of metastatic tumors in bone, brain and liver, and reduced the survival periods (Fig. 3F–I and Supplemental Fig. 4H). Therefore, these results indicated that HLF-downexpressing NSCLC cells possess stronger ability of local colonization and growth, as well as distant metastasis.

3.4. HLF represses growth of NSCLC cells under low nutritional condition

We further investigated the biological function of HLF in NSCLC using CCK-8, colony formation and Annexin apoptosis assays, and found that the proliferation and apoptotic ability of NSCLC cells were not significantly affected by HLF in normal culture conditions (Supplemental Fig. 5A–C). However, upregulating HLF repressed, while silencing HLF promoted anchorage-independent and suspension growth capability of NSCLC cells (Fig. 4A and B), indicating that silencing HLF augmented the capacity of NSCLC cells to survive under suspension conditions, namely anoikis resistance, a major hallmark of metastatic cancer cells implicated in distant metastasis in a variety of cancers [23–25]. Furthermore, our results showed that upregulating HLF increased, while silencing HLF decreased the pH level of the culture medium, although the phenotype and number of NSCLC cells were not influenced by HLF in normal condition (Supplemental Fig. 5D). These

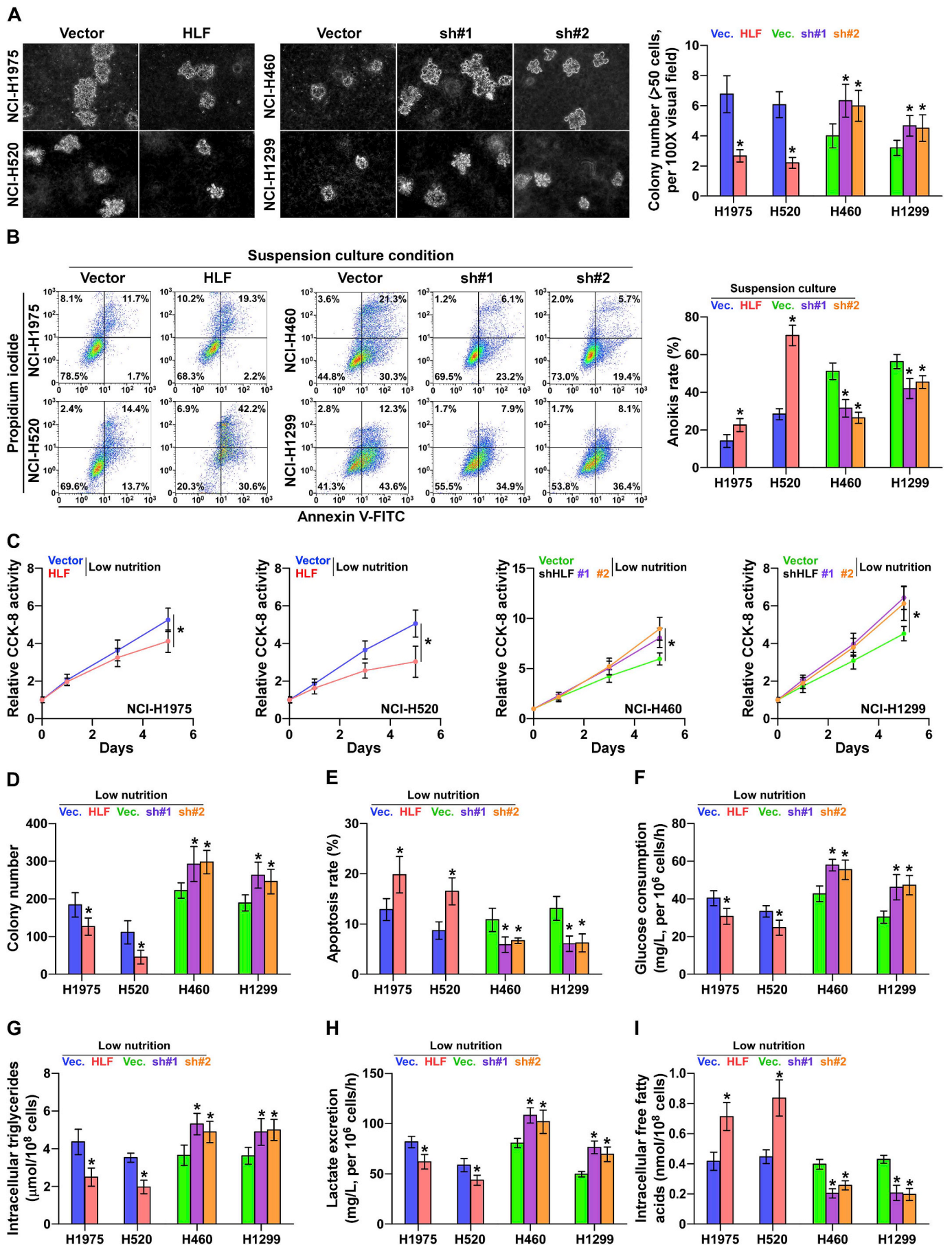
findings suggested that downexpression of HLF may promote the adaption of NSCLC cells to low nutritional condition through the nutrition metabolic pathway, since cancer cells preferably metabolize through the anaerobic route even in normal oxygenic conditions [26]. In fact, dysregulation of circadian genes led to metabolic dysregulation in NSCLC [22], and HLF has been widely implicated in several material metabolic processes, including lipid [27] and oxidative metabolism [28]. Interestingly, our results further revealed that HLF overexpression inhibited proliferation but increased the apoptotic potential in NSCLC cells, and vice versa under the low nutritional condition, which consisted of low-serum (1%) and low-glucose (1 g/L) cultured medium (Fig. 4C–E). Therefore, these findings suggested that HLF was implicated in the nutrition metabolism of the culture medium in which cancer cells grow, which is prerequisite for the repressive effect of HLF on growth of NSCLC cells.

3.5. Downexpression of HLF promotes anaerobic metabolism in NSCLC cells

To further determine the specific metabolic pathway affected by HLF in NSCLC cells, the effect of HLF on glucose, fatty acid and proteins was examined under low nutritional condition. As shown in Supplemental Fig. 6A, altered expression of HLF did not affect the total protein contents. However, upregulating HLF decreased consumption of glucose, triglycerides and secretion of lactate, but increased the free fatty acid level (Fig. 4F–I). Paradoxically, upregulating HLF increased total intracellular ATP production and LDH activity (Supplemental Fig. 6B and C). These findings suggested that under low nutritional condition, HLF-overexpressing cancer cells are more prone to aerobic metabolism rather than anaerobic metabolism, which was further supported by the findings that upregulating HLF reduced activity of lactic dehydrogenase (LDH), a rate-limiting enzyme in anaerobic glycolysis, and several anaerobic glycolysis and lactate fermentation-related gene, but enhanced multiple tricarboxylic acid cycle-related genes (Supplemental Fig. 6D and E). Conversely, silencing HLF exhibited an opposite effect on metabolic characteristics, which promoted anaerobic metabolism in NSCLC cells (Fig. 4F–I and Supplemental Fig. 6C and D). Indeed, cancer cells exhibit altered glucose metabolism characters with a preference for anaerobic metabolism even when the oxygen content is normal, a phenomenon termed “Warburg effect” [26]. Collectively, our results indicated that downexpression of HLF promotes the conversion of preferred metabolic pathway from tricarboxylic acid cycle to anaerobic metabolism in NSCLC cells, which further promotes cell growth under low nutritional condition.

3.6. HLF activates PPAR α and PPAR γ and inhibits NF- κ B/p65 signaling

To further determine the underlying mechanism mediating the inhibitory role of HLF in the growth and metastasis of NSCLC under low nutritional condition, luciferase reporter plasmids of multiple signaling pathways were transfected into NSCLC cells. As shown in Fig. 5A, upregulating HLF dramatically enhanced the activity of PPAR signaling, and repressed the activity of NF- κ B signaling in NSCLC cells; conversely, silencing HLF yielded an opposite effect (Fig. 5A). Gene Set Enrichment Analysis (GSEA) was performed based on HLF expression in the NSCLC dataset from TCGA, and the result showed that HLF expression levels positively correlated with PPAR signaling, but negatively with NF- κ B signaling (Supplemental Fig. 6F). Furthermore, HLF



(caption on next page)

Fig. 4. HLF represses growth and anaerobic metabolism of NSCLC cells under low nutritional condition. (A) Upregulating HLF repressed, while silencing HLF promoted anchorage-independent growth capability of NSCLC cells. $*P < 0.05$. (B) Upregulating HLF promoted, while silencing HLF repressed apoptosis of NSCLC cells under suspension growth. $*P < 0.05$. (C and D) Overexpression of HLF repressed, while downregulation of HLF enhanced the proliferation ability of NSCLC cells cultured under low nutritional condition in CCK-8 assay and colony formation assay. $*P < 0.05$. (E) Overexpression of HLF enhanced, while downregulation of HLF repressed apoptosis of NSCLC cells cultured under low nutritional condition via Annexin V apoptosis assay. $*P < 0.05$. (F to I) In low nutritional condition, upregulating HLF decreased consumption of glucose (F), triglyceride (G) and secretion of lactate (H), and increased the intracellular free fatty acid (I), while downregulation of HLF had opposite effects. $*P < 0.05$.

expression was significantly associated with lipid oxidation and glycolysis according to GSEA analysis (Supplemental Fig. 6F). Importantly, several lines of evidence reported that HLF was implicated in translocation and activation of PPAR by increasing lipolysis-induced free fatty acid accumulation [27], which further inactivates NF- κ B signaling that has been extensively implicated in the progression and metastasis of cancers via disrupting the binding to p65 to target DNA [18,29,30]. PPAR signaling was constituted of several family members, including PPAR α , PPAR β/δ and PPAR γ . Therefore, it is crucial to determine the specific PPAR member involved in the inhibitory effect of HLF on NF- κ B signaling, as well as on tumorigenesis and metastasis of NSCLC. First, the expression levels of PPAR α , PPAR β/δ and PPAR γ were examined in ten paired NSCLC tissues. As shown in Supplemental Fig. 6G and H, PPAR α expression was significantly downregulated in 4/10 paired tissues, PPAR γ in 8/10; by contrast, PPAR β/δ was upregulated in 8/10 tissues. PPAR α and PPAR γ have been extensively reported to function as tumor-suppressive signaling in NSCLC [31–33], while PPAR β/δ reportedly plays an oncogenic role [34]. Consistently, Western blot analysis revealed that upregulating HLF increased total PPAR α and PPAR γ expression and nuclear translocation and increased expression of I κ B α , but decreased total and nuclear levels of phosphorylated NF- κ B and p65 (Fig. 5B). Conversely, silencing HLF exerted the opposite role (Fig. 5B). Therefore, our results revealed that HLF activates PPAR α and PPAR γ , and inhibits NF- κ B/p65 signaling in NSCLC.

3.7. PPAR α /PPAR γ /NF- κ B/p65 signaling mediates the functional role of HLF in NSCLC

We further investigated the significance of the PPAR α /PPAR γ /NF- κ B/p65 signaling axis in the functional role of HLF in NSCLC cells using PPAR α agonist Fenofibrate [35], PPAR γ agonist Pioglitazone [33] and NF- κ B signaling inhibitors LY2409881 [36]. Our result showed that PPAR activity was robustly upregulated by Fenofibrate and Pioglitazone, but not by LY2409881 in HLF-silenced cells (Fig. 5C). However, Fenofibrate, Pioglitazone and LY2409881 differentially reduced the activity of NF- κ B signaling in HLF-silenced cells (Fig. 5D). Importantly, the stimulatory effect of HLF downexpression on cell anchorage-independent growth and anti-anoikis ability was attenuated by Fenofibrate, Pioglitazone and LY2409881 (Fig. 5E and F). Conversely, Fenofibrate, Pioglitazone and LY2409881 reversed the pro-proliferative (clonal growth) and anti-apoptotic effects of HLF downregulation in NSCLC cells under low nutrition conditions (Fig. 5G and H). Additionally, we further silenced PPAR α in HLF-overexpressing cells, and found that individually silencing PPAR α and PPAR γ reduced PPAR activity (Supplemental Fig. 7A), increased the activity of NF- κ B signaling (Supplemental Fig. 7B), anchorage-independent growth, anti-anoikis and proliferation ability of HLF-overexpressing cells (Supplemental Fig. 7C–E), but reduced apoptotic ratio (Supplemental Fig. 7F). Importantly, we found that LY2409881 reversed the pro-proliferative (clonal growth) and anti-apoptotic effects mediated by PPAR α and PPAR γ downregulation in HLF-overexpressing cells (Supplemental Fig. 7C–F). Furthermore, Fenofibrate and Pioglitazone could attenuate the increased glucose uptake and lactate release in NSCLC cells with HLF downregulation (Supplemental Fig. 7G and H). However, LY2409881 had no significant effect on glucose uptake and lactate release in NSCLC cells with HLF downregulation (Supplemental Fig. 7G and H). Taken together, our findings indicated that HLF suppresses

proliferation and promote anoikis and apoptosis of NSCLC cells by inhibiting NF- κ B/p65 signaling by enhancing the activity of PPAR α and PPAR γ in low nutrition condition.

3.8. Genetic deletion and methylation contribute to downexpression of HLF

To determine the underlying mechanism contributing to the downexpression of HLF in NSCLC, we first analyzed the levels of copy number variation (CNV) of HLF in NSCLC dataset from TCGA and our 20 NSCLC tissues. We detected deletion of HLF in 9.4% (95/1007) NSCLC tissues, amplification in 41.9% (422) and normal diploid in 48.7% (490) in TCGA dataset (Supplemental Fig. 8A) and deletion in 15% (3/20) and amplification in 35% (7/20) of our samples (Supplemental Fig. 8H and I). However, statistical significance of HLF expression was only observed between tissues with deletions and those with diploid, but not in tissues with amplification (Supplemental Fig. 8B). Since genetic deletion was only identified in a minority of the NSCLC tissues, we speculated that other unknown mechanisms may be likely involved in HLF downexpression in NSCLC tissues. Therefore, we further analyzed the methylation array dataset for NSCLC from TCGA using multiple methylation probes, and found hypermethylation of HLF in NSCLC tissues compared with that in the matched ANT (Supplemental Fig. 8C). Due to defective CpG islands in HLF, we hypothesized that the methylation level of the CpG sites affects RNA polymerase II (Pol II, POLR2A) transcriptional activity and dynamics at the POLR2A-DNA binding domain, based on previous report [37,38]. Through analyzing the bioinformatics' data from UCSC Genome Browser, we identified that the presence of multiple methylation sites, including probes 8–12, in the body of Pol II (Supplemental Fig. 8D), prompting us to infer that hypermethylation levels of these sites resulting in the reduced transcription of HLF and subsequently decreased the expression of HLF in NSCLC tissues. Based on this hypothesis, the number of methylated sites in each tissue was further evaluated using five independent methylation probes, including cg01392772, cg05452524, cg02383154, cg01185682 and cg01451391 (methylated status of each probe was scored 1 with the highest score being 5). As shown in Supplemental Figure 8E, 24.3% (198/815) of NSCLCs harbored differential methylation, in which 5.4% (44) tissues were found with score 1 methylated site, 10.1% (88) with score 2, 4.3% (35) with score 3, 2.1% (17) with score 4 and 2.5% (20) with score 5. Moreover, methylation was found in 35.0% (7/20) of our samples (Supplemental Fig. 8J and K). To comprehensively evaluate the combined effect of CNV and methylation levels on HLF expression in NSCLC, we proposed a scoring standard that integrated the CNV and methylation score (CNV & Methy Score), in which the percentages of different scores in NSCLC tissues were calculated and presented (Supplemental Fig. 8F). Then, the HLF expression levels in NSCLC tissues with different scores were further compared. As shown in Supplemental Fig. 8G, with increasing score, the HLF expression was gradually decreased in NSCLC tissues. Consistently, a strong and negative correlations between the HLF CNV & Methy score and mRNA and proteins levels of HLF was demonstrated in our NSCLC samples (Fig. 6A–C). These findings indicated that deletion and methylation levels cooperatively contribute to downexpression of HLF in NSCLC tissues. Furthermore, our results further demonstrated that PPAR α and PPAR γ expression levels were upregulated, and NF- κ B/p65 expression was downregulated in HLF-overexpressing NSCLC tissues; conversely, HLF-downexpressing NSCLC tissues presented low

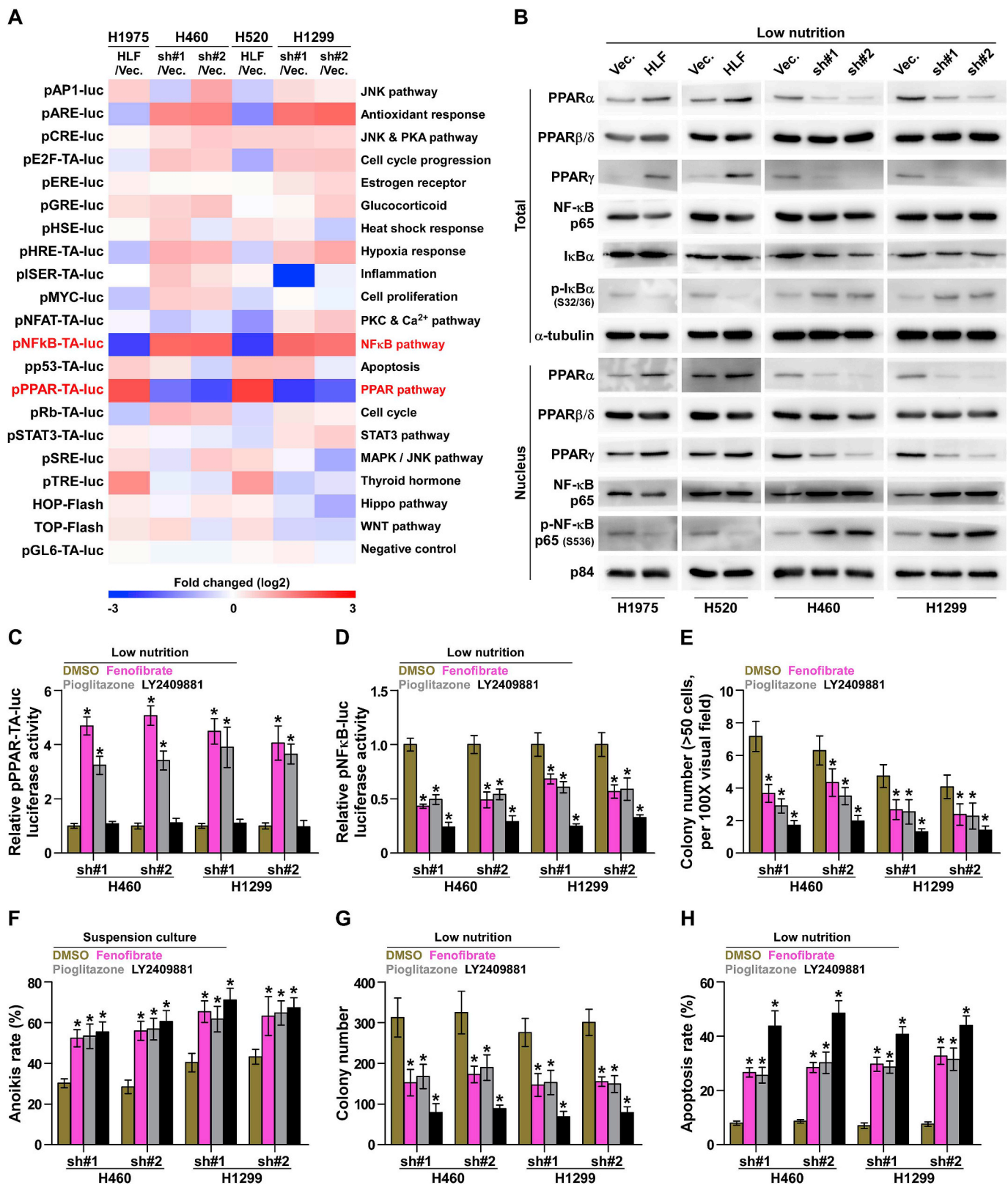


Fig. 5. HLF suppresses proliferation and promote anoikis and apoptosis of NSCLC cells by inhibiting NF-κB/p65 signaling via enhancing activity of PPARα and PPARγ. (A) Activity of luciferase reporter constructs of several signaling pathway were examined in the HLF-overexpressing or –silencing NSCLC cells. (B) The effects of HLF on nuclear translocation of total and nuclear PPARα, PPARβ/δ and PPARγ expression, p-NF-κB/p65 and p-IκBα and IκBα expression in NSCLC cells under low nutrition. α-Tubulin and p84 served as the cytoplasmic and nuclear loading controls, respectively. (C) Luciferase activity of PPAR was robustly upregulated by PPARα agonist Fenofibrate (20 μm) and PPARγ agonist Pioglitazone (10 μm), but not by NF-κB signaling inhibitors LY2409881 (10 μm) in HLF-silenced cells. *P < 0.05. (D) Fenofibrate, Pioglitazone and LY2409881 differentially reduced the activity of NF-κB signaling in HLF-silenced cells. *P < 0.05. (E and F) Fenofibrate, Pioglitazone and LY2409881 inhibited capabilities of anchorage-independent growth and anti-anoikis in HLF-silenced cells. *P < 0.05. (G and H) Clonal growth and apoptosis in HLF-silenced cells was increased by Fenofibrate, Pioglitazone and LY2409881 under low nutrition. *P < 0.05. Each bar represents the mean values ± SD of three independent experiments.

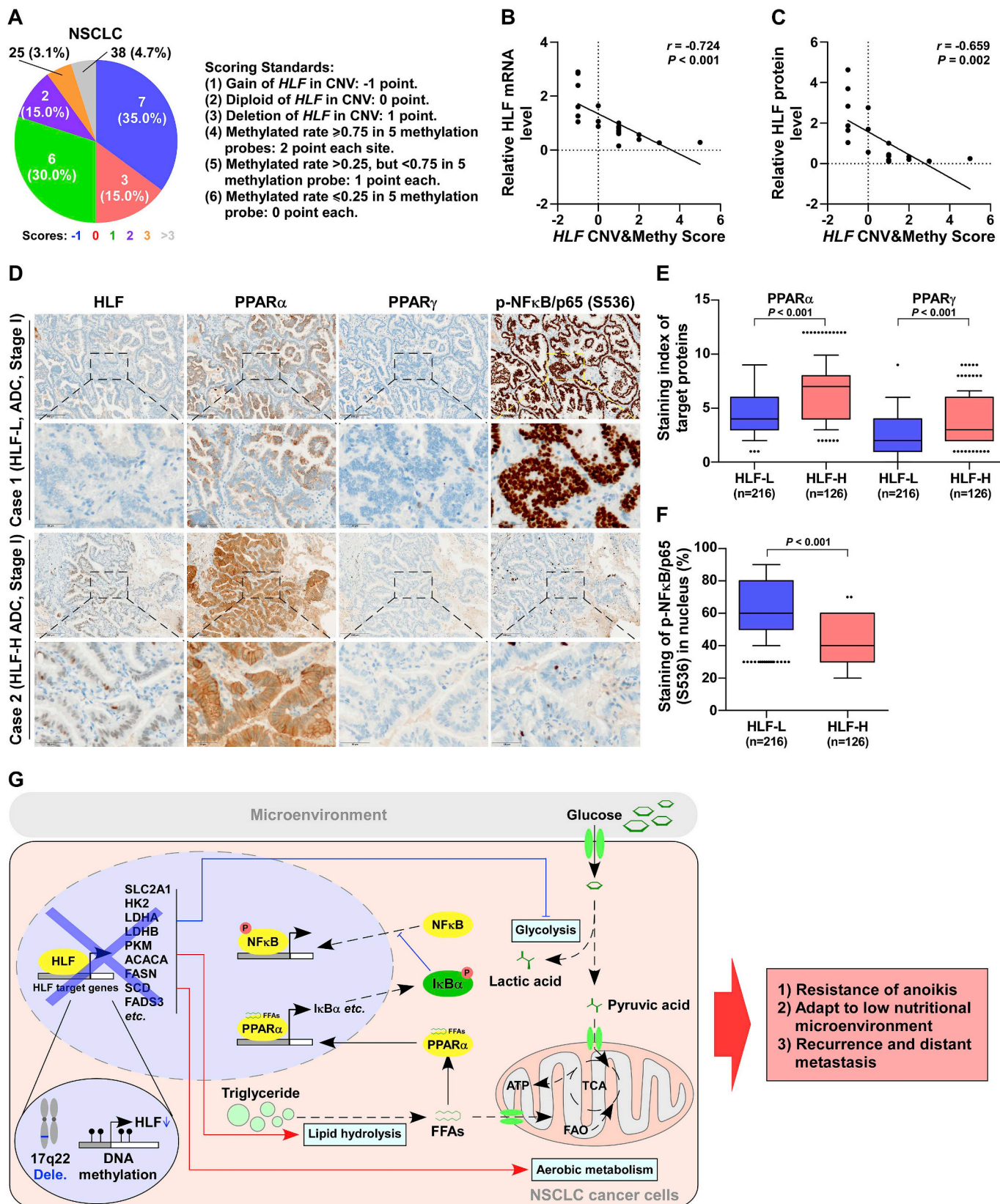


Fig. 6. HLF expression negatively correlates with copy number variation and methylation. (A) Scores combined effect of CNV and methylation levels of HLF in ANT and tumors of 20 NSCLC patients. (B and C) Correlations between CNV & methylation scores of HLF and mRNA (B) and proteins (C) levels in NSCLC tissues. (D–F) HLF expression levels were positively correlated with expression levels of PPAR α and PPAR γ , but negatively associated with activity of NF- κ B/p65 in NSCLC specimens. Left panel (D): two representative cases of HLF overexpression and downexpression are shown. Right panel (E and F): expression levels of PPAR α , PPAR γ and p-NF- κ B/p65 in HLF-overexpressing and downexpressing NSCLC tissues. (G) Schematic illustration displays that downexpression of HLF promotes anaerobic metabolism through regulating PPAR α /p65/NF- κ B signaling contributes to distant metastasis in NSCLC.

PPAR α and PPAR γ levels and high activity of p-NF- κ B/p65 (Fig. 6D–F). In conclusion, our results reveal that downregulation of HLF caused by both DNA deletion and methylation activates NF- κ B signaling by attenuating the activity of PPAR α and PPAR γ , which further promotes anaerobic metabolism to support anoikis resistance of NSCLC cells under low nutritional condition, and ultimately induce NSCLC recurrence and distant metastasis (Fig. 6G).

4. Discussion

As a member of the proline and acid rich bZIP transcription factor family (PAR bZIP) [13,14], HLF plays an important physiological role in the development of the nervous system [39] and apoptosis of fibroblasts [40,41]. Furthermore, aberrant expression of HLF has been extensively implicated in the development and progression of multiple human cancer types: HLF was downregulated in hematological malignancy [42–44] and glioma [45], and promoted proliferation, metastasis and therapeutic resistance of cancer cells. By contrast, overexpression of HLF promoted anchorage-independent growth of human basal cell carcinoma [46] and aggravated sorafenib resistance of hepatocellular carcinomas by upregulating OCT4 and SOX2 in a positive feedback loop [47]. These findings suggested that the opposite and even paradoxical role of HLF is tumor-type dependent. However, the clinical significance and roles of HLF in NSCLC remain largely unknown. To the best of our knowledge, we demonstrated for the first time that in this study, HLF was downregulated in NSCLC tissues, which predicted early relapse and progression, as well as multiple organs distant metastasis in NSCLC patients. Our results further demonstrated that downexpression of HLF promoted anaerobic metabolism to support anchorage-independent growth of NSCLC cells under low nutritional condition, which further promoted lung colonization and metastasis of NSCLC cells to bone, liver and brain *in vivo*. Mechanistic investigation revealed that HLF inhibited NF- κ B signaling by increasing the activity and nuclear translocation of PPAR α and PPAR γ , which further repressed the growth of NSCLC cells. Taken together, our results indicated that HLF plays a crucial anti-tumor role in the progression and metastasis of NSCLC.

It has been well documented that circadian rhythms regulators hold favorable prospect as a potential prognostic marker in a variety of cancers. In their study, Climent et al. has shown that deletion-induced downexpression of PER3 predicted early recurrence and poor prognosis in breast cancer patients, particularly in the estrogen receptor (ER)-positive subset [48]. Furthermore, Papagiannakopoulos et al. reported that dysregulation of the circadian genes PER2 and BMAL1 promoted lung tumor growth by increased c-MYC expression and predicted poor progression-free survival in NSCLC patients [22]. In the current study, our results showed that HLF was downregulated in NSCLC tissues, which was significantly and positively correlated with early relapse and distant metastasis in NSCLC patients. Furthermore, *in vivo* lung colonization and left cardiac ventricle inoculation models showed that downregulating HLF dramatically increased lung colonization and outgrowth, and metastasis ability of NSCLC cells to the bone, liver and brain. Therefore, our findings indicated that HLF may serve as a novel prognostic marker in NSCLC.

Mechanistically, HLF exerts its biological function through PPAR signaling [30]. Consistently, our results demonstrated that HLF enhanced the activity and promoted the nuclear translocation of PPAR α and PPAR γ in NSCLC cells. Importantly, the pro-tumorigenic role of HLF downexpression in NSCLC was significantly abrogated by Fenofibrate and Pioglitazone respectively, as evidenced by reduced proliferation and increased apoptosis of the NSCLC cells. Several lines of evidence have shown that PPAR α and PPAR γ played an anti-tumor role in the growth and progression of NSCLC [31–33,49]. However, increased level of PPAR α has been implicated in the carcinogenesis of liver [50]. This difference suggested that PPAR α signaling plays an opposite, even paradoxical role in different human cancer types, which may, in part, be explained by the different response of different cancer cells to

PPAR α . In fact, the possibility that PPAR α agonist can be safely used for the prevention and treatment of NSCLC has been confirmed by two independent studies [31,32]. Therefore, our results suggested that in HLF-downexpressing NSCLC, administration of PPAR α agonist may be useful as a therapeutic modality to suppress the metastasis of NSCLC. However, further studies are warranted in a study with a larger sample size.

A great deal of attention has focused on the role of anaerobic metabolism in the development, progression and metastasis of cancers [26]. In the current study, downregulation of HLF promoted anaerobic metabolism by PPAR α /PPAR γ signaling as indicated by the finding that Fenofibrate and Pioglitazone attenuated the increased glucose uptake and lactate release in NSCLC cells, which further promoted anchorage-independent growth, proliferation and anoikis resistance of NSCLC cells under low nutritional condition. In fact, PPAR signaling has been reported to play an important role in several metabolic pathway, including glucose, lipid, cholesterol [27]. However, LY2409881 had no significant effect on glucose uptake and lactate release in NSCLC cells with HLF downregulation. These findings supported the hypothesis that repression of PPAR α /PPAR γ signaling contributed to HLF downexpression-induced anaerobic metabolism in NSCLC cells, which further promotes cell growth under low nutritional condition.

In summary, our results reveal that downregulation of HLF caused by both deletion and methylation activates NF- κ B signaling by attenuating the activity of PPAR α and PPAR γ , which further promotes anaerobic metabolism to support anchorage-independent growth of NSCLC cells under low nutritional condition, and subsequent lung colonization and distant metastasis. Therefore, the current study presents key novel findings concerning the critical roles and underlying mechanism of HLF in NSCLC, which will facilitate the development of anti-metastatic therapeutic strategy against NSCLC.

Author contributions

Xin Zhang and Yanming Huang conceived the project and drafted the manuscript. Jiarong Chen, Aibin Liu and Zhichao Lin conducted the experiments and contributed to the analysis of data. Bin Wang, Xingxing Chai and Shasha Chen performed the animal experiments. Yan Zheng, Minyan Wu and Lin Xiao analyzed the informatics data. Wenjie Lu, Mingzhu Zheng, Ting Cao and Ronggang Li performed IHC and the analysis of data., Wenguang Pang, Wenhai Huang, Xiangmeng Chen, Wansheng Long, Meigong Zhong and Qiong chen conducted the patient information's organizing. Daren Lin, Zhihui Wang, Zhuming Lu and Fangyong Lei contributed to the cell biology and molecular biology experiments. Jincheng Zeng, Dong Ren and Jun Li edited and revised the manuscript. All authors discussed the results and approved the manuscript.

Declaration of competing interest

We wish to confirm that there are no known conflicts of interest associated with this publication and there has been no significant financial support for this work that could have influenced its outcome.

Acknowledgements

This study was supported by the grants from the National Natural Science Foundation of China (81902941, 81802918, 81702917), the China Postdoctoral Science Foundation Grant (2019M660206, 2019M653210, 2019M653218), the Science and Technology Project of Guangdong Province (2019A1515011246, 2019A1515011565, 2018A030310007), the Natural Science Foundation of Hunan Province (2019JJ50970), the Medical Science Foundation of Guangdong Province (B2020104, B2018239, A2017103), the Science Foundation of Guangdong Province Bureau of Traditional Chinese Medicine

(20181273), the Science and Technology Project of Jiangmen (2019-252-2-1, 2019030102430012905, 2019030102480013011, 2018090106380023859), the Medical Science Foundation of Jiangmen Central Hospital (J201901, J201801) and “Group-type” Special Supporting Project for Educational Talents in Universities (4SG19221, 4SG19210).

Appendix A. Supplementary data

Supplementary data to this article can be found online at <https://doi.org/10.1016/j.canlet.2020.04.007>.

References

- [1] F. Bray, J. Ferlay, I. Soerjomataram, R.L. Siegel, L.A. Torre, A. Jemal, Global cancer statistics 2018: GLOBOCAN estimates of incidence and mortality worldwide for 36 cancers in 185 countries, *Ca - Cancer J. Clin.* 68 (2018) 394–424.
- [2] M. Riihimäki, A. Hemminki, M. Fallah, H. Thomsen, K. Sundquist, J. Sundquist, K. Hemminki, Metastatic sites and survival in lung cancer, *Lung Canc. Res.* 86 (2014) 78–84.
- [3] C.L. Chaffer, R.A. Weinberg, A perspective on cancer cell metastasis, *Science* 331 (2011) 1559–1564.
- [4] C. Savvidis, M. Koutsilieris, Circadian rhythm disruption in cancer biology, *Mol. Med.* 18 (2012) 1249–1260.
- [5] S.J. Kuo, S.T. Chen, K.T. Yeh, M.F. Hou, Y.S. Chang, N.C. Hsu, J.G. Chang, Disturbance of circadian gene expression in breast cancer, *Virchows Arch. Int. J. Pathol.* 454 (2009) 467–474.
- [6] B. Fekry, A. Ribas-Latre, C. Baumgartner, J.R. Deans, C. Kwok, P. Patel, L. Fu, R. Berdeaux, K. Sun, M.G. Kolonin, S.H. Wang, S.H. Yoo, F.M. Sladek, K. Eckel-Mahan, Incompatibility of the circadian protein BMAL1 and HNF4alpha in hepatocellular carcinoma, *Nat. Commun.* 9 (2018) 4349.
- [7] C.M. Yeh, J. Shay, T.C. Zeng, J.L. Chou, T.H. Huang, H.C. Lai, M.W. Chan, Epigenetic silencing of ARNTL, a circadian gene and potential tumor suppressor in ovarian cancer, *Int. J. Oncol.* 45 (2014) 2101–2107.
- [8] M. Qiu, Y.B. Chen, S. Jin, X.F. Fang, X.X. He, Z.F. Xiong, S.L. Yang, Research on circadian clock genes in non-small-cell lung carcinoma, *Chronobiol. Int.* 36 (2019) 739–750.
- [9] B. Liu, K. Xu, Y. Jiang, X. Li, Aberrant expression of Per1, Per2 and Per3 and their prognostic relevance in non-small cell lung cancer, *Int. J. Clin. Exp. Pathol.* 7 (2014) 7863–7871.
- [10] R. Xiang, Y. Cui, Y. Wang, T. Xie, X. Yang, Z. Wang, J. Li, Q. Li, Circadian clock gene Per2 downregulation in nonsmall cell lung cancer is associated with tumour progression and metastasis, *Oncol. Rep.* 40 (2018) 3040–3048.
- [11] B. Chen, Y. Tan, Y. Liang, Y. Li, L. Chen, S. Wu, W. Xu, Y. Wang, W. Zhao, J. Wu, Per2 participates in AKT-mediated drug resistance in A549/DDP lung adenocarcinoma cells, *Oncology Lett.* 13 (2017) 423–428.
- [12] X. Zhang, L. Zhang, B. Lin, X. Chai, R. Li, Y. Liao, X. Deng, Q. Liu, W. Yang, Y. Cai, W. Zhou, Z. Lin, W. Huang, M. Zhong, F. Lei, J. Wu, S. Yu, X. Li, S. Li, Y. Li, J. Zeng, W. Long, D. Ren, Y. Huang, Phospholipid Phosphatase 4 promotes proliferation and tumorigenesis, and activates Ca(2+)-permeable Cationic Channel in lung carcinoma cells, *Mol. Canc.* 16 (2017) 147.
- [13] J.M. Ferrell, J.Y. Chiang, Circadian rhythms in liver metabolism and disease, *Acta Pharm. Sin.* B 5 (2015) 113–122.
- [14] E. Reszka, S. Zienoldiddin, Epigenetic basis of circadian rhythm disruption in cancer, *Methods Mol. Biol.* 1856 (2018) 173–201.
- [15] H. Liu, D. Huang, D.L. McArthur, L.G. Boros, N. Nissen, A.P. Heaney, Fructose induces transketolase flux to promote pancreatic cancer growth, *Canc. Res.* 70 (2010) 6368–6376.
- [16] X. Wu, X. Zhang, L. Yu, C. Zhang, L. Ye, D. Ren, Y. Li, X. Sun, L. Yu, Y. Ouyang, X. Chen, L. Song, P. Liu, X. Lin, Zinc finger protein 367 promotes metastasis by inhibiting the Hippo pathway in breast cancer, *Oncogene* 39 (2020) 2568–2582.
- [17] X. Zhang, D. Ren, L. Guo, L. Wang, S. Wu, C. Lin, L. Ye, J. Zhu, J. Li, L. Song, H. Lin, Z. He, Thymosin beta 10 is a key regulator of tumorigenesis and metastasis and a novel serum marker in breast cancer, *Breast Cancer Res.* 19 (2017) 15.
- [18] X. Zhang, D. Ren, X. Wu, X. Lin, L. Ye, C. Lin, S. Wu, J. Zhu, X. Peng, L. Song, miR-1266 contributes to pancreatic cancer progression and chemoresistance by the STAT3 and NF-kappaB signaling pathways, molecular therapy, *Nucl. Acids* 11 (2018) 142–158.
- [19] S. Huang, Q. Wa, J. Pan, X. Peng, D. Ren, Q. Li, Y. Dai, Q. Yang, Y. Huang, X. Zhang, W. Zhou, D. Yuan, J. Cao, Y. Li, P. He, Y. Tang, Transcriptional downregulation of miR-133b by REST promotes prostate cancer metastasis to bone via activating TGF-beta signaling, *Cell Death Dis.* 9 (2018) 779.
- [20] D. Ren, Y. Dai, Q. Yang, X. Zhang, W. Guo, L. Ye, S. Huang, X. Chen, Y. Lai, H. Du, C. Lin, X. Peng, L. Song, Wnt5a induces and maintains prostate cancer cells dormancy in bone, *J. Exp. Med.* 216 (2019) 428–449.
- [21] K.A. Le Cao, F. Rohart, L. McHugh, O. Korn, C.A. Wells, YuGene: a simple approach to scale gene expression data derived from different platforms for integrated analyses, *Genomics* 103 (2014) 239–251.
- [22] T. Papagiannakopoulos, M.R. Bauer, S.M. Davidson, M. Heimann, L. Subbaraj, A. Bhutkar, J. Bartlebaugh, M.G. Vander Heiden, T. Jacks, Circadian rhythm disruption promotes lung tumorigenesis, *Cell Metabol.* 24 (2016) 324–331.
- [23] M. Haemmerle, M.L. Taylor, T. Gutschner, S. Pradeep, M.S. Cho, J. Sheng, Y.M. Lyons, A.S. Nagaraja, R.L. Dood, Y. Wen, L.S. Mangala, J.M. Hansen, R. Rupaimoole, K.M. Gharpure, C. Rodriguez-Aguayo, S.Y. Yim, J.S. Lee, C. Ivan, W. Hu, G. Lopez-Berestein, S.T. Wong, B.Y. Karlan, D.A. Levine, J. Liu, V. Afshar-Kharghan, A.K. Sood, Platelets reduce anoikis and promote metastasis by activating YAP1 signaling, *Nat. Commun.* 8 (2017) 310.
- [24] C.L. Buchheit, K.J. Weigel, Z.T. Schafer, Cancer cell survival during detachment from the ECM: multiple barriers to tumour progression, *Nat. Rev. Canc.* 14 (2014) 632–641.
- [25] Y. Tang, J. Pan, S. Huang, X. Peng, X. Zou, Y. Luo, D. Ren, X. Zhang, R. Li, P. He, Q. Wa, Downregulation of miR-133a-3p promotes prostate cancer bone metastasis via activating PI3K/AKT signaling, *J. Exp. Clin. Oncol. Res.* 37 (2018) 160.
- [26] M.G. Vander Heiden, L.C. Cantley, C.B. Thompson, Understanding the Warburg effect: the metabolic requirements of cell proliferation, *Science* 324 (2009) 1029–1033.
- [27] F. Gachon, N. Leuenberger, T. Claudel, P. Gos, C. Jouffe, F. Fleury Olela, X. de Mollerat du Jeu, W. Wahli, U. Schibler, Proline- and acidic amino acid-rich basic leucine zipper proteins modulate peroxisome proliferator-activated receptor alpha (PPARalpha) activity, *Proc. Natl. Acad. Sci. U. S. A.* 108 (2011) 4794–4799.
- [28] F. Gachon, F.F. Olela, O. Schaad, P. Descombes, U. Schibler, The circadian PAR-domain basic leucine zipper transcription factors DBP, TEF, and HLF modulate basal and inducible xenobiotic detoxification, *Cell Metabol.* 4 (2006) 25–36.
- [29] D. Ren, Q. Yang, Y. Dai, W. Guo, H. Du, L. Song, X. Peng, Oncogenic miR-210-3p promotes prostate cancer cell EMT and bone metastasis via NF-kappaB signaling pathway, *Mol. Canc.* 16 (2017) 117.
- [30] Y. Jung, J.C. Kim, Y. Choi, S. Lee, K.S. Kang, Y.K. Kim, S.N. Kim, Eupatilin with PPARalpha agonistic effects inhibits TNFalpha-induced MMP signaling in HaCat cells, *Biochem. Biophys. Res. Commun.* 493 (2017) 220–226.
- [31] S.P. Lakshmi, A.T. Reddy, A. Banno, R.C. Reddy, PPAR Agonists for the Prevention and Treatment of Lung Cancer vol. 2017, PPAR research, 2017, p. 8252796.
- [32] N. Skrypnik, X. Chen, W. Hu, Y. Su, S. Mont, S. Yang, M. Gangadhariah, S. Wei, J.R. Falck, J.L. Jat, R. Zent, J.H. Capdevila, A. Pozzi, PPARalpha activation can help prevent and treat non-small cell lung cancer, *Canc. Res.* 74 (2014) 621–631.
- [33] N. Srivastava, R.K. Kollipara, D.K. Singh, J. Sudderth, Z. Hu, H. Nguyen, S. Wang, C.G. Humphries, R. Carstens, K.E. Huffman, R.J. DeBerardinis, R. Kitterl, Inhibition of cancer cell proliferation by PPARgamma is mediated by a metabolic switch that increases reactive oxygen species levels, *Cell Metabol.* 20 (2014) 650–661.
- [34] X. Zuo, W. Xu, M. Xu, R. Tian, M.J. Moussalli, F. Mao, X. Zheng, J. Wang, J.S. Morris, M. Gagea, C. Eng, S. Kopetz, D.M. Maru, A. Rashid, R. Broaddus, D. Wei, M.C. Hung, A.K. Sood, I. Shureiqi, Metastasis regulation by PPAR expression in cancer cells, *JCI insight* 2 (2017) e91419.
- [35] D. Rigano, C. Sirignano, O. Tagliatalata-Scafati, The potential of natural products for targeting PPARalpha, *Acta Pharm. Sin.* B 7 (2017) 427–438.
- [36] C. Deng, M. Lipstein, R. Rodriguez, X.O. Serrano, C. McIntosh, W.Y. Tsai, A.S. Wasmuth, S. Jaken, O.A. O'Connor, The novel IKK2 inhibitor LY2409881 potently synergizes with histone deacetylase inhibitors in preclinical models of lymphoma through the downregulation of NF-kappaB, *Clin. Canc. Res. Off. J. Am. Assoc. Canc. Res.* 21 (2015) 134–145.
- [37] H. Takeshima, S. Yamashita, T. Shimazu, T. Niwa, T. Ushijima, The presence of RNA polymerase II, active or stalled, predicts epigenetic fate of promoter CpG islands, *Genome Res.* 19 (2009) 1974–1982.
- [38] Z. Gao, H.L. Liu, L. Daxinger, O. Pontes, X. He, W. Qian, H. Lin, M. Xie, Z.J. Lorkovic, S. Zhang, D. Miki, X. Zhan, D. Pontier, T. Lagrange, H. Jin, A.J. Matzke, M. Matzke, C.S. Pikaard, J.K. Zhu, An RNA polymerase II- and AGO4-associated protein acts in RNA-directed DNA methylation, *Nature* 465 (2010) 106–109.
- [39] J.K. Hitzler, H.D. Soares, D.W. Drolet, T. Inaba, S. O'Connell, M.G. Rosenfeld, J.I. Morgan, A.T. Look, Expression patterns of the hepatic leukemia factor gene in the nervous system of developing and adult mice, *Brain Res.* 820 (1999) 1–11.
- [40] A. Ritchie, O. Gutierrez, J.L. Fernandez-Luna, PAR bZIP-bik is a novel transcriptional pathway that mediates oxidative stress-induced apoptosis in fibroblasts, *Cell Death Differ.* 16 (2009) 838–846.
- [41] K. Suzuki, K. Yoshida, T. Ueha, K. Kaneshiro, A. Nakai, N. Hashimoto, K. Uchida, T. Hashimoto, Y. Kawasaki, N. Shibamura, N. Nakagawa, Y. Sakai, A. Hashiramoto, Methotrexate upregulates circadian transcriptional factors PAR bZIP to induce apoptosis on rheumatoid arthritis synovial fibroblasts, *Arthritis Res. Ther.* 20 (2018) 55.
- [42] S. Garg, A. Reyes-Palomares, L. He, A. Bergeron, V.P. Lavalley, S. Lemieux, P. Gendron, C. Rohde, J. Xia, P. Jagdhane, C. Muller-Tidow, D.B. Lipka, S. Imren, R.K. Humphries, C. Waskow, B. Vick, I. Jeremias, G. Richard-Carpentier, J. Hebert, G. Sauvageau, J.B. Zaugg, F. Barabe, C. Pabst, Hepatic leukemia factor is a novel leukemic stem cell regulator in DNMT3A, NPM1, and FLT3-ITD triple-mutated AML, *Blood* 134 (2019) 263–276.
- [43] M. Wahlestedt, V. Ladopoulos, I. Hidalgo, M. Sanchez Castillo, R. Hannah, P. Sawen, H. Wan, M. Dudenhofer-Pfeifer, M. Magnusson, G.L. Norddahl, B. Gottgens, D. Bryder, Critical modulation of hematopoietic lineage fate by hepatic leukemia factor, *Cell Rep.* 21 (2017) 2251–2263.
- [44] J. Roychoudhury, J.P. Clark, G. Gracia-Maldonado, Z. Unnisa, M. Wunderlich, K.A. Link, N. Dasgupta, B. Aronow, G. Huang, J.C. Mulloy, A.R. Kumar, MEIS1 regulates an HLF-oxidative stress axis in MLL-fusion gene leukemia, *Blood* 125 (2015) 2544–2552.
- [45] S. Chen, Y. Wang, C. Ni, G. Meng, X. Sheng, HLF/miR-132/TTK axis regulates cell proliferation, metastasis and radiosensitivity of glioma cells, *Biomed. Pharmacotherapy* 83 (2016) 898–904.
- [46] K.M. Waters, R. Tan, L.K. Opreško, R.D. Quesenberry, S. Bandyopadhyay,

- W.B. Chrisler, T.J. Weber, Cellular dichotomy between anchorage-independent growth responses to bFGF and TPA reflects molecular switch in commitment to carcinogenesis, *Mol. Carcinog.* 48 (2009) 1059–1069.
- [47] O. Musso, N. Beraza, Hepatocellular carcinomas: evolution to sorafenib resistance through hepatic leukaemia factor, *Gut* 68 (2019) 1728–1730.
- [48] J. Climent, J. Perez-Losada, D.A. Quigley, I.J. Kim, R. Delrosario, K.Y. Jen, A. Bosch, A. Lluch, J.H. Mao, A. Balmain, Deletion of the PER3 gene on chromosome 1p36 in recurrent ER-positive breast cancer, *J. Clin. Oncol. : Off. J. Am. Soc. Clin. Oncology* 28 (2010) 3770–3778.
- [49] S.S. Hann, F. Zheng, S. Zhao, Targeting 3-phosphoinositide-dependent protein kinase 1 by N-acetyl-cysteine through activation of peroxisome proliferators activated receptor alpha in human lung cancer cells, the role of p53 and p65, *J. Exp. Clin. Canc. Res. : CR (Clim. Res.)* 32 (2013) 43.
- [50] F.J. Gonzalez, J.M. Peters, R.C. Cattley, Mechanism of action of the nongenotoxic peroxisome proliferators: role of the peroxisome proliferator-activator receptor alpha, *J. Natl. Cancer Inst.* 90 (1998) 1702–1709.